Comparative Analysis of Water Body Extraction Accuracy Based on Thresholding Method

Linjiang Lou [1] , Chen Chen [1], Minmin Li [1], Kun Liu [1]

[1] Land Satellite Remote Sensing Application Center, MNR ,Beijing, China- llj910808@hotmail.com,
410208288@qq.com; 289256678@qq.com; 283940896@qq.com

KEY WORDS: SPOT4, MNDWI, Thresholding Method, Water Body Extraction, Image Segmentation.

Abstract

With the continuous development of remote sensing technology, various methods for land water body extraction based on satellite remote sensing have emerged. The thresholding method, as a commonly used image segmentation technique, possesses advantages such as high efficiency and wide applicability, making it widely employed in water body extraction research. In this thesis, utilizing SPOT4 imagery, we conducted experimental comparisons of water body extraction using the Iteration thresholding algorithm, Kittler-Illingworth (KI) thresholding algorithm, and Otsu thresholding algorithm. The experimental results demonstrate that all three thresholding methods exhibit good performance in water body extraction, with the Kittler-Illingworth (KI) thresholding algorithm achieving the highest relative accuracy.

1. Introduction

Satellite remote sensing technology, with its unique advantages such as wide coverage and periodic revisit, has been widely applied in various domains, including water resource investigation monitoring (Pu,Jingjuan,1992), With the improvement of remote sensing technology and its extensive application, methods for extracting thematic information from remote sensing data have been continuously advancing. Various techniques such as thresholding (Lu, K. K.and Li, S. H. 1992), differencing, ratioing, density slicing, chromatic discrimination, ratio estimation (Chen, W. R. and Kuo, D. F., 1995), spectral relationship analysis (Yu, Guangming et al., 1996), as well as knowledge-based automatic water body discrimination methods and shape-based water body recognition and classification methods have been proposed and applied. Natural water bodies exhibit significantly higher absorption of electromagnetic waves in the range of 0.4 to 2.5 μm compared to most other land cover types, resulting in lower overall radiance levels observed in water bodies compared to other land cover types, which manifests as darker tones in colour remote sensing images. In the infrared spectrum, water absorbs more energy than in the visible spectrum. Even shallow water absorbs almost all incident energy in the near-infrared and mid-infrared bands. Therefore, the reflected energy of water in these bands is minimal, while vegetation and soil exhibit lower absorption and higher reflection characteristics in these bands (Du Jinkang et al.,2001). Based on these characteristics, Various kinds of optical bands and spectral indexes are used in previous studies. Near-infrared appears as a popular band used to detect water. The famous Normalized Differential Water Index (NDWI) is proposed based on the near-infrared band. Many researchers applied this band on water detection. (Smith,1997) noticed the phenomena that flooding areas have low reflectivity in near-infrared band and researched the flood area detection problem with single data and a time series analysis. However, metropolis roads and building roofs have low reflectivity in the near-infrared band and likewise influence the water monitoring. (McFeeter,1996). proposed the Normalized Difference Water Index (NDWI) based on green and near-infrared bands by Landsat satellite images. The NDWI index presents good performance in extracting water regions. (Xu,2005) modified the NDWI proposed by McFeeter, and proposed the modified NDWI (MNDWI) by introducing the middle-infrared band. (Carlson et al.,1994) proposed the Normalized Difference Vegetation Index (NDVI). As the NDVI of water is negative while the vegetation and soil are comparatively high, the NDVI could be used to detect the water area. (Cao et al., 2005) pointed out SWIR band could discriminate water and shadows by using the thresholding method in SWIR band and build an auto-extraction decision tree model. NDVI is also a widely used index. (Wang et al. , 2002) conducted the flood monitoring by two temporal Landsat/TM images, one before the disaster and one during the disaster, and pointed out that the vegetation covered area is ignored by only the TM4 (760-900nm, SWIR) and TM7 bands (2080-2350nm, LWIR).

The pixel-level thresholding is always based on the histogram thresholding method. (Yuan Xinzhi et al， 2016) proposed a method based on the Otsu algorithm for locally adaptive threshold determination and conducted water body extraction experiments on the Minjiang River Basin using the NDWI index from environmental small satellite imagery. (Xi Xiaoyan et al,2009) utilized Landsat-7 ETM+ data and proposed a method combining spectral relationships and thresholding, achieving good extraction results and effectively reducing misclassification. (Pan Yue. and Zhang Liting,2015) found that the thresholding method is more suitable for water body extraction in plain areas. They compared the advantages and limitations of the thresholding method, spectral relationship method, and index method in water body extraction in both plain and mountainous areas based on Landsat 8 OLI imagery and object-oriented thinking. (Xu Rong et al.,2015) used Landsat TM imagery and employed two thresholding algorithms, namely, maximum between-class variance and iteration, to determine the thresholds for water body extraction in several commonly used lakes. (Ren Chao and Liu, Tao-Lin, 2022) addressed the issues of low universality and difficulty in obtaining optimal thresholds for water body extraction from remote sensing images. They proposed a combination of the Cuckoo Search algorithm and Otsu method, forming the Cuckoo Otsu adaptive threshold search method. (Chen Wenqian et al.,2015) conducted water body information extraction in the Tekes River Basin using single-

band thresholding, NDWI, and multi-band methods, analysing the advantages and disadvantages of the three extraction methods. (Yikun Li et al., 2013) Based on the multi-peak grayscale histogram thresholding algorithm, the process begins by smoothing the histogram using a mean filter to eliminate minor fluctuations while retaining significant peaks and valleys that reflect the overall trend of the histogram. Subsequently, local maxima and minima in the histogram are identified to determine appropriate thresholds. Through experimental studies involving automated extraction of water bodies from Landsat TM images, the automatic threshold selection algorithm proves effective for batch processing in extracting remote sensing information of water bodies and other land cover features, yielding favourable extraction outcomes. (Feyisa et al., 2014) proposed a new spectral index AWEI, which improved the classification accuracy in areas that include shadow and dark surfaces. AWEI is the arithmetic combinations of several spectral bands which are selected to maximize the separability of water and non-water surfaces. (Zhao et al., 2003) proposed an iterative mixed analysis method and analysed the spectral characters in different bands by the CBERS-1 data, which in the procedure of iterative mixed analysis, the sampled points are selected manually based on prior knowledge.

To summarize the water index method and the automatic threshold selection method in image analysis have long been attracting the attention of numerous scholars. The common goal is to find a simple, practical, and adaptive approach that emphasizes automatic threshold selection. With three relatively common thresholding methods, the representative algorithms by statistical models are Iterative thresholding algorithm (Fornasier, M., Rauhut, H, 2008), Kittler-Illingworth (KI) thresholding algorithm (Kittler, J. and J. Illingworth, 1986), and Otsu thresholding algorithm (Otsu, N., 1979).

Through comparing these three prevalent algorithmic models, the goal is to determine the most effective thresholding algorithm for extracting water bodies from SPOT-4 data. This algorithm will be applicable not only for routine water extraction but also for tasks such as estimating the affected area in flood disaster scenarios.

2. Study Area And Data

Cagayan de Oro is a large port city of the Philippines located in the southern part of the Philippines. The central coordinates of the image of the test area are N8° 30' 58"N, E124° 40' 51"E. The remote sensing data selected in this paper is SPOT4 optical image with the resolution of 20 meters. The experimental data were acquired on July 14th 2011with band 2 (B), band 3 (G), band 4 (G) and band 11 (SWIR).

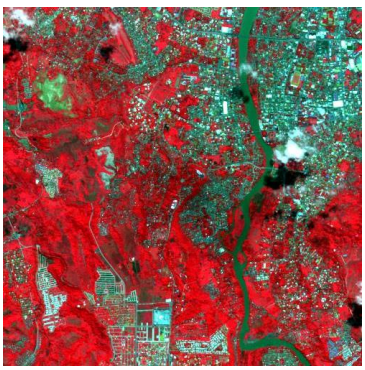

Figure 1 Test area of image data

In this paper, the improved normalized index MNDWI could not only extract water bodies within the range of cities and towns, but also easily distinguish shadows and water bodies. Moreover, it solved the difficult problem of removing shadows in water extraction. The calculation formula is as follows:

$$MNDWI = \frac{(\rho(Green) - \rho(SWIR))}{(\rho(Green) + \rho(SWIR))} \quad (1)$$

Figure 2 MNDWI image data

Figure 3 Water body reference image

3. Methods

3.1 Otsu Thresholding Algorithm

The Otsu thresholding algorithm is also called the maximum between-class variance algorithm. This standpoint is motivated by a conjecture that well threshold classes would be separated in gray-levels, and conversely, a threshold giving the best separation of classes in gray-levels would be the best threshold.

Suppose the pixels of a figure be represented in L gray levels, 1, 2, ..., L. The number of pixels at level i is denoted by n_i and the total number of pixels by $N = n_1 + n_2 + \ldots + n_L$ The gray-level histogram is normalized and regarded as a probability distribution:

$$p_i = \frac{n_i}{N} \quad \sum_{i=1}^{L} p_i = 1 \quad p_i \geq 0 \quad (2)$$

Dichotomizing all the pixels into two classes C_0 and C_1 by a threshold at level k, the probabilities of class occurrence and class mean value are given by:

$$\omega_0 = \sum_{i=1}^{k} p_i = \omega(k) \tag{3}$$

$$\omega_1 = \sum_{i=k+1}^{L} p_i = 1 - \omega(k) \tag{4}$$

And

$$\mu_0 = \sum_{i=1}^{k} \frac{ip_i}{\omega_0} = \mu(k)/\omega(k) \tag{5}$$

$$\mu_1 = \sum_{i=k+1}^{L} ip_i/\omega_1 = \frac{\mu_T - \mu(k)}{1-\omega(k)} \tag{6}$$

μ_0 and μ_1 are the zeroth and the first-order cumulative moments of the histogram up to the kth level, respectively, and

$$\mu_t = \mu(L) = \sum_{i=1}^{L} ip_i \tag{7}$$

μ_t is the total mean level of the original figure.

The object function (the criterion measures) in the Otsu thresholding algorithm is:

$$\eta = \sigma_B^2/\sigma_T^2 \tag{8}$$

Where

$$\sigma_B^2 = \omega_0(\mu_0 - \mu_T)^2 + \omega_1(\mu_1 - \mu_T)^2 \tag{9}$$

$$\sigma_T^2 = \sum_{i=1}^{L}(i - \mu_T)^2 p_i \tag{10}$$

The optimal threshold k^* that maximizes η is selected in the following sequential search by using the simple cumulative quantities:

$$\eta(k) = \sigma_B^2(k)/\sigma_T^2 \tag{11}$$

$$\sigma_B^2(k) = \frac{[\mu_T\omega(k) - \mu(k)]^2}{\omega(k)[1-\omega(k)]} \tag{12}$$

and the optimal threshold k^* is

$$\sigma_B^2(k^*) = \max_{1\le k<L} \sigma_B^2(k) \tag{13}$$

3.2 Kittler-Illingworth Thresholding Algorithm

The Kittler-Illingworth(KI) thresholding algorithm has been adopted, which has been used in remote sensing image analysis predominantly in modified versions for automatic change detection in difference or (log) ratio data. As a global parametric thresholding technique, the KI algorithm uses a minimum error approach to group the sets of pixels of gray-scale images into object and background classes and assumes the image histogram h(g) gives the frequency of occurrence of the various levels of g to be the only available information about the image. The histogram is treated as an estimate of the class-conditional probability density functions in a mixture of two clusters. The histograms of the selected images are assumed to be modelled statistically by two 1-D normal distributions of the semantic classes "water" and "non-water" p(g|i)i = 1: water, 2: non−water, with parameters mean value μ_i standard deviation σ_i and a priori probability and a priori probability P_i so that:

$$p(g) = \sum_{i=1}^{2} P_i p(g|i) \tag{14}$$

where

$p(g|i) = \frac{1}{\sqrt{2\pi}\sigma_i} e^{-\frac{(g-\mu_i)^2}{2\sigma_i^2}}$ by comparing their gray-levels under the threshold T, the cost function measures the cost in misclassifying pixels. For each brightness value, the fitting criterion *J(T)* is calculated. As long as threshold T is varied, the models of the Gaussian distributions change, correspondingly. The better the model fits the data; the lower is the criterion of this cost function. Therefore, the brightness value T is selected as the optimal threshold τ_{KI} , where the classification error is minimized according to the Bayes classification rule, namely the number of pixels that are mis-classified is the smallest:

$$\tau_{KI} = \arg\min_T J(T) \tag{15}$$

3.3 Iterative Thresholding Algorithm

The basic theory of the self-adjustment Iterative thresholding algorithm is the function approximation theory. The main steps are:
(1) The optical image was classified into two groups by assuming an initial cache region and selecting the initial thresholding value T1. The groups with the gray value larger than T1. are G_1, while the groups with the gray value smaller than T1 are G_2.

(2) The mean value of G_1 and G_2 is μ_1 and μ_2, respectively. Then (2) the new thresholding value $T_2=(\mu_1+\mu_2)/2$ is obtained.

(3) If $|T_2 - T_1| < T_0$, then T is the global thresholding value, otherwise T would be assigned to T_0, and continue acquire the thresholding gray value until $|T_2 - T_1| < T_0$.

The flow chart of this algorithm is shown as Figure 4:

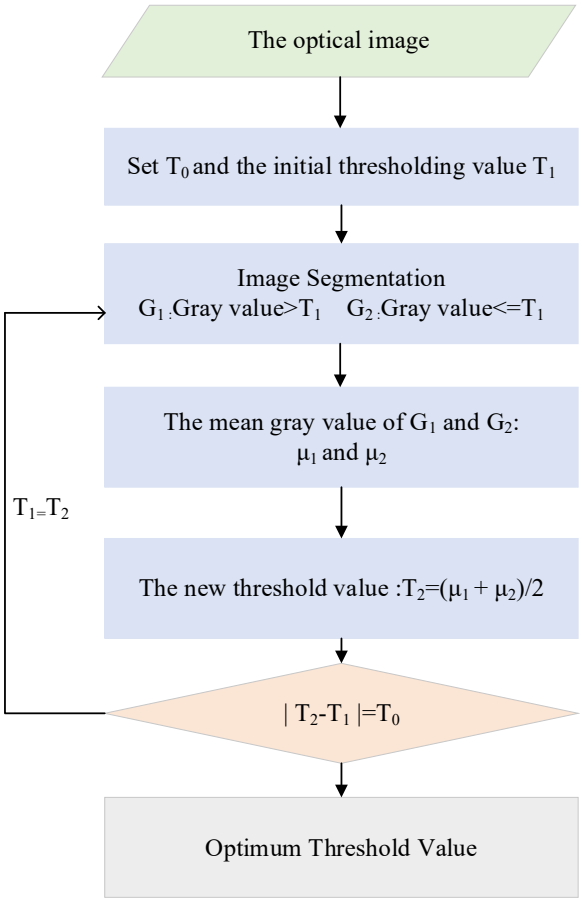

Figure 4 The flow chart of the iteration thresholding algorithm

4. Result

4.1 Water Extraction Results

This thesis compares the effectiveness of three commonly used thresholding methods for water body extraction based on MNDWI data. The Otsu thresholding algorithm yielded a threshold value of 0.23 (shown in Figure 5).

Figure 5 Ostu Thresholding Algorithm segmentation result

The Kittler-Illingworth Thresholding Algorithm produced a threshold value of 0.21 (shown in Figure 6).

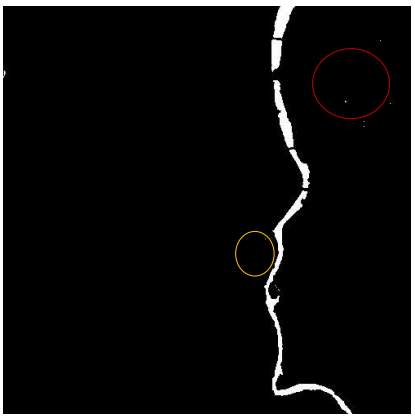

Figure 6 KI Thresholding Algorithm segmentation result

The Iteration Thresholding Algorithm resulted in a threshold value of 0.28 (shown in Figure 7).

Figure 7 Iterative Thresholding Algorithm segmentation result

As depicted in the figures, both the Otsu thresholding algorithm and the Kittler-Illingworth Thresholding Algorithm performed well in water body extraction, but they faced challenges in distinguishing certain shadow areas (highlighted in red) and recognizing small rivers (highlighted in yellow). The Iteration Thresholding Algorithm exhibited a lower error rate but also a higher rate of missed detections.

The design and evaluation of detection algorithms is often facilitated by assuming some meaningful probability distributions for the target and clutter. For each measurement X, there are two possibilities: target absent or present. Assigning the hypothesis for target absent as H_0, correspondingly, the hypothesis for target present is H_1. As shown in the table, for each measurement X, there are four decisions (Beck, J. Robert, and Edward K. Shultz,1986).

	H_0	H_1
H_0	A: Don't Report	B: False Alarm
H_1	C:Missed Detection	D: Detection

Table 1. For each measurement x, there are four decisions

There is always a compromise between choosing a low threshold to increase the probability of (target) detection P_D and a high threshold to keep the probability of false alarm P_{FA} low. Based

on Table 1 the probability of detection, $P_D = \frac{D}{C+D}$, and the probability of false alarm, $P_{FA} = \frac{B}{A+B}$.

Ostu thresholding algorithm is a detection rate of 79.11% and a false alarm rate of 0.045%.

		Ostu	
		Others	Water
Truth	Others	244345	111
	Water	1158	4386
P_D		0.7911	
P_{FA}		0.00045	

Table 2. Detection Rate and False Alarm Rate of Ostu thresholding algorithm

Kittler-Illingworth thresholding algorithm is a detection rate of 81.37% and a false alarm rate of 0.06%.

		KI	
		Others	Water
Truth	Others	244309	147
	Water	1033	4511
P_D		0.8137	
P_{FA}		0.0006	

Table 3. Detection Rate and False Alarm Rate of Kittler-Illingworth thresholding algorithm

Iterative thresholding algorithm is a detection rate of 73.07% and a false alarm rate of 0.26% .

		Iterative	
		Others	Water
Truth	Others	244345	64
	Water	1158	4051
P_D		0.7307	
P_{FA}		0.0026	

Table 4. Detection Rate and False Alarm Rate of Iterative thresholding algorithm

4.2 Accuracy Evaluation

To compare the detection performance among different thresh-olding methods quantitively, we introduced the index of Figure of Merit (Foulkes and Dooth, 2000).

The results show that the FoM of Otsu thresholding algorithm is 0.9945, the FoM of KI Thresholding Algorithm is 0.9947, and the FoM of Iterative Thresholding Algorithm is 0.9935.

	Ostu	KI	Iterative
P_D	0.7307	0.8137	0.7307
P_{FA}	0.0026	0.0006	0.0026
FOM	0.9945	0.9947	0.9935

Table 5. FoM results for the three thresholding algorithms

5. Conclusion

This thesis compares the performance of three thresholding methods for water body extraction using MNDWI data and achieves satisfactory results. These methods can be applied in scenarios that require rapid extraction, such as water resource investigation, monitoring, and flood monitoring. Among the three methods, the Kittler-Illingworth thresholding algorithm exhibits the best performance, although there may still be cases of misclassification in certain image shadow areas.

Acknowledgements

The authors would like to thank Chen Chen of Land Satellite Remote Sensing Application Center, MNR as corresponding author for equally important efforts related to this work.

References

Pu, Jingjuan (1992). Principles and Methods of Visual Interpretation of Remote Sensing Images. China Science and Technology Press.

Lu, K. K. & Li, S. H. (1992). Improvement of water body identification technique for Tm data. *Journal of Remote Sensing* (1), 17-23.

Chen, W. R., Kuo, D. F. (1995). Application of ratio synthesis and feature principal component selection techniques in extracting oil area information. *Remote Sensing Technology and Applications*, 10(3), 7.

Yu, Guangming, Wang, Chaonan, Zhong, Rugang, Zou, Shanghui, Zhang, Jinxia, Zhao, Junhua (1996). Dem-based flood information extraction and loss estimation. *Remote Sensing of Land Resources* (1), 9.

Du Jinkang, Huang YS, Feng XZ, Wang ZL. (2001). A study on water body extraction method and classification of Spot satellite imagery. *Journal of Remote Sensing*, 5(3), 6.

Smith, S. M. and Brady, J. M. (1997). Susan—a new approach to low level image processing. *International Journal of Computer Vision*, 23(1), 45-78.

McFeeters, S. K. (1996). The use of the Normalized Difference Water Index (NDWI) in the delineation of open water features. *International Journal of Remote Sensing*, 17(7), 1425-1432.

Han-Qiu, X. U. (2005). A study on information extraction of water body with the modified normalized difference water index (mndwi). *Journal of Remote Sensing*.

Toby, N., Carlson, Robert, R., Gillies, et al. (1994). A method to make use of thermal infrared temperature and ndvi measurements to infer surface soil water content and fractional vegetation cover. *Remote Sensing Reviews*.

Cao, K., Jiangnan, X. Li, H. Lu (2005). Research on automatic extraction model of urban water bodies based on spot-5 images. *Remote Sensing of Land Resources (*4), 5.

Wang, Y., Colby, J. D., and Mulcahy, K. A. (2002). An efficient method for mapping flood extent in a coastal flood plain using Landsat TM and DEM data, *International Journal of Remote Sensing* 23(18).

Yuan, Xinzhi Yuan, Jiang Hong, Yunzhi Chen, Xiaoqin Wang (2016). An adaptive threshold water body extraction method applying Otsu method. *Remote Sensing Information* , 31(5), 7.

Xi, Xiaoyan, Shen, Nan, Li, Xiaojuan (2009). Research on water body extraction method of Etm+ image. *Computer Engineering and Design* (4), 4.

Pan Yue and Zhang Liting (2015). Comparative study of several commonly used water body extraction methods based on oli images.*Jiangxi Science*, 33(5), 6.

Xu Rong, Zhao Chunzhe, Xiong Jiang (2015) Comparative study of several lake water body remote sensing extraction algorithms.

Ren Chao and Liu, TaoLin (2022). An Adaptive Thresholding Method for Otsu Cuckoo for Water Body Extraction. Science of Surveying and Mapping.

Chen, W. C., Ding, J. L., Li, Y. H., Niu, Z. Yi (2015). Water body extraction method based on domestic gf-1 remote sensing images. *Resource Science*, 37(6), 1166-1172.

Yikun Li, Shuwen Yang, Tao Liu (2013). Automatic threshold selection algorithm for remote sensing images based on multi-peak histogram. *Journal of Lanzhou Jiaotong University*, 32(6), 6.

Feyisa, G. L., Meilby, H., Fensholt, R., Proud, S. R. (2014). Automated Water Extraction Index: A new technique for surface water mapping using Landsat imagery. *Remote Sensing of Environment*, 140, 23-35.

Otsu, N. (1979). A threshold selection method from gray-level histograms, *IEEE Transactions on Systems, Man, and Cybernetics*, 9: 62-66.

Kittler, J. and J. Illingworth (1986). Minimum error thresholding Pattern Recognition, 19: 41-47.

Fornasier, M. & Rauhut, H. (2008). Iterative thresholding algorithms. *Applied & Computational Harmonic Analysis*, 25(2), 187-208.

Beck, J. R. & Shultz, E. K. (1986). The use of relative operating characteristic (roc) curves in test performance evaluation. *Archives of Pathology & Laboratory Medicine*, 110(1), 13.

Foulkes, S.B. and D.M. Dooth (2000). Ship detection in ERS and Radarsat imagery using a self-organising Kohonen neural network, Proc. of Nova Scotia Conference on Ship Detection in Coastal Waters, Digby, NS, Canada